

On the Application of Numerical Methods to Hallén’s Equation: The Case of a Lossy Medium

Christos Mystilidis, Panagiotis J. Papakanellos,
George Fikioris, *Senior Member, IEEE*, and Themistoklis K. Mavrogordatos

arXiv:2001.06080v1 [physics.comp-ph] 16 Jan 2020

Abstract—A previous paper analyzed in detail the difficulties associated with the application of numerical methods to Hallén’s integral equation with the approximate kernel for the case of a lossless surrounding medium. The present paper extends to the case where the medium is conducting and points out similarities and differences between the two cases. Our main device is an analytical/asymptotic study of the antenna of infinite length.

Index Terms—Antenna theory, antennas in matter, integral equations, moment methods, wire antennas

I. INTRODUCTION

The purpose of the 2001 paper [1] is to analyze the difficulties associated with the numerical solution of the usual (Hallén and Pocklington) integral equations for a thin-wire transmitting antenna. In [1], the antenna is isolated in a lossless medium, is perfectly conducting, and is center-driven by a delta-function generator. For the case of the well-known approximate (also called reduced) kernel, the main difficulties arise from the fact that neither of the said integral equations has a solution; the important issue of “nonsolvability” is discussed in detail in [1]–[3]. Since 2001, the analysis of [1] has been extended in a number of directions, including the so-called “extended thin-wire kernel” [4], feeds other than the delta-function generator [5]–[8], loop antennas [9], [10], a similar equation of electrostatics [11], as well as antennas with finite conductivity, including carbon-nanotube antennas [12]. Furthermore, the analysis of [1] forms the foundation for the development of an easy-to-apply technique [11], [13]–[16] that is an *a posteriori* remedy for the most important difficulties.

The present article extends results of [1] toward a different direction, specifically to the case where the medium surrounding the thin-wire antenna is conducting. A standard general reference for such antennas is [17], while [18] contains moment-method analyses, and the recent paper [19] is a pertinent application to carbon nanotubes. Section II contains straightforward numerical results that explicate the difficulties associated with moment-method solutions. Then, in Section III, we explain the findings of Section II by means of an analytical study of the much simpler antenna of infinite length.

C. Mystilidis and G. Fikioris are with the School of Electrical and Computer Engineering, National Technical University of Athens, GR 157-73 Zografou, Athens, Greece (e-mail: christosmy96@hotmail.com, gfiki@ece.ntua.gr).

P. J. Papakanellos is with the Department of Aeronautical Sciences, Hellenic Air Force Academy, Dekelia Air Force Base, Athens 13671, Greece (email: papakanellos@yahoo.gr).

T. K. Mavrogordatos is with the Department of Physics, Stockholm University, SE-106 91, Stockholm, Sweden (email: themis.mavrogordatos@fysik.su.se).

Most of the derivations pertaining to Section III are in the Appendix, whose contents parallel material in [1].

The approximate kernel, which is a much simpler version of the so-called exact kernel, is extensively used alongside its “exact” counterpart, featuring in the majority of modern antenna textbooks; see, e.g., [20]–[23]. Furthermore, extensions of the integral equations with the approximate kernel apply to more involved “real-life” antenna configurations, which are typically dealt with by standard antenna-analysis software such as the popular Numerical Electromagnetics Code (NEC) [24]. Let us add that the approximate kernel enjoys wide popularity in the literature dealing with Hallén’s and Pocklington’s equations for carbon nanotube antennas (CNTs). Characteristic examples include [25]–[27], where the approximate kernel is used exclusively, while in other works both kernels are employed (e.g., [28], [29]).

It is perhaps to be expected that the difficulties we find in this paper are quite different from the difficulties (discussed recently in [12], [16]) that arise in the case where the antenna itself is an imperfect conductor [30], [31]. On the other hand, it is probably surprising that our central analytical result for the infinite antenna—eqn. (8) below—appears very similar to the corresponding result of [1] for the case of a lossless surrounding medium; compare our (8) to eqn. (38) of [1]. The predictions of the two results, however, are not the same. This is why our derivations and discussions focus on the similarities/differences with [1].

We close this Introduction by listing the main conclusions from [1]: For the case of a lossless surrounding medium and for $N \gg 1$, where $2N + 1$ is the number of subdomain basis functions, the moment-method solutions for the current $I(z)$ exhibit large and unphysical oscillations near the driving point at $z = 0$. These oscillations specifically occur in the imaginary part $\text{Im}\{I(z)/V\}$ (V is the driving voltage at $z = 0$), while the real part presents no such oscillations. Additional oscillations, in both the real and imaginary parts, occur near the antenna endpoints. The oscillations are not due to roundoff or matrix-ill-conditioning effects. Rather, they are due to the aforementioned “nonsolvability,” discussed particularly clearly in [2]. Condition numbers are large and thus magnify roundoff errors [5], but these are separate issues. The near field associated with the oscillating currents [11], [13]–[16] exhibits a superdirective-type behavior, oscillating up to a radial distance ρ equal to the antenna radius a . After $\rho = a$, the oscillations cease and the field is similar to that produced by the current satisfying the exact integral equation. This similarity, in fact, forms the basis for the *a posteriori*

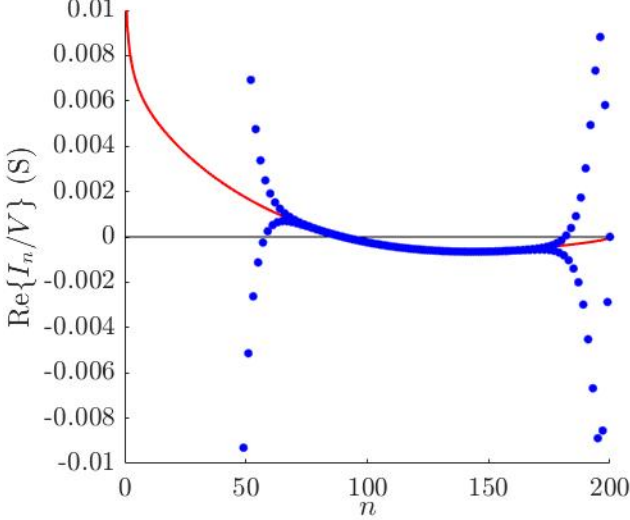


Fig. 1. Real part of I_n/V (dots) as calculated by Galerkin's method; $\epsilon = \epsilon_0$, $\mu = \mu_0$, $\omega = 2\pi \times 5 \times 10^8$ rad/s, $\gamma = 0.1$ S/m, $h = 0.25\lambda$, $a = 0.007022\lambda$, and $N = 200$. Some values near $n = 0$ are out of scale and are not shown. The solid lines are corresponding results with the exact kernel.

remedy mentioned previously.

II. DIFFICULTIES ASSOCIATED WITH FINITE ANTENNA

The current $I(z)$ on a wire antenna center-driven by a delta-function generator satisfies Hallén's equation [17], [32], [33]

$$\int_{-h}^h K(z - z') I(z') dz' = \frac{iV}{2\zeta_c} \sin k_c |z| + C \cos k_c z, \quad |z| < h \quad (1)$$

where

$$K(z) = \frac{1}{4\pi} \frac{\exp(ik_c \sqrt{z^2 + a^2})}{\sqrt{z^2 + a^2}} \quad (2)$$

In (1) and (2), $K(z)$ is the approximate kernel, $2h$ and $2a$ are the antenna length and diameter, C is a constant to be determined from $I(\pm h) = 0$ (see [17] for discussions on this condition), and an $e^{-i\omega t}$ time dependence is assumed. The complex parameters k_c and ζ_c are

$$k_c = \omega \sqrt{\mu \epsilon_c}, \quad \zeta_c = \sqrt{\frac{\mu}{\epsilon_c}}, \quad \epsilon_c = \epsilon + i \frac{\gamma}{\omega} \quad (3)$$

in which the real parameters ϵ , μ , and γ are the permittivity, permeability, and conductivity of the surrounding medium. While standard in the literature, we stress that (1) is approximate due to current leakage into the lossy surrounding medium [32]. In (1) and (2), the differences from [1] (whose figures pertain to a lossless medium with $\gamma = 0$) appear in ζ_c and k_c , which now have nonzero imaginary parts, assumed to satisfy $\text{Im}\{k_c\} > 0$ and $\text{Im}\{\zeta_c\} < 0$.

Let $\epsilon = \epsilon_0$, $\mu = \mu_0$, $\lambda = 2\pi c/\omega$, $c = 3 \times 10^8$ m/s, $\omega = 2\pi f = 2\pi \times 5 \times 10^8$ rad/s, and $\gamma = 0.1$ S/m. At the aforementioned frequency f , our chosen value of γ corresponds to damp native soil from Kirtland Air Force Base (and is also close to the value for wet Belen soil) [34]. Also, let $h = 0.25\lambda$, $a = 0.007022\lambda$, and $N = 200$; these three parameters are the same as in Figs. 1 and 2 of [1], with $2N+1$

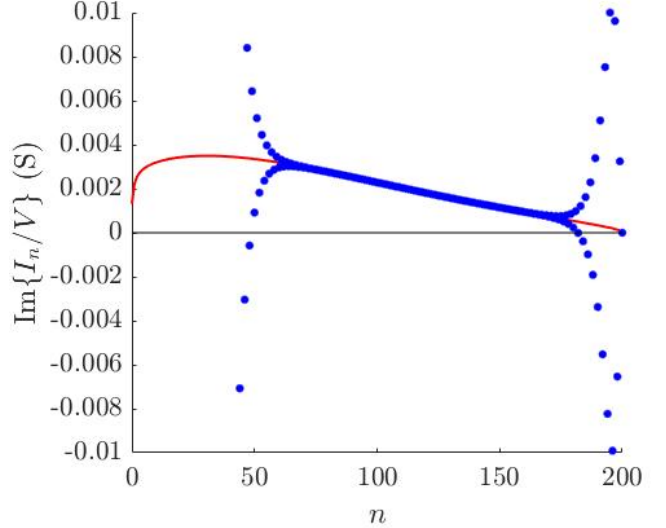


Fig. 2. Like Fig. 1, but for imaginary part of I_n/V .

being the number of pulse basis functions. When applied to (1), Galerkin's method gives the results shown in Figs. 1 and 2, where the abscissa n denotes the basis-function number, with $n = 0$ at the driving point $z = 0$. Corresponding results with the exact kernel are also shown. Our Galerkin's method is identical to the lossless case and is described in detail in [1]. The difference with the corresponding figures in [1] is immediately apparent: Oscillations near the driving point occur not only in $\text{Im}\{I(z)/V\}$, but also in the real part $\text{Re}\{I(z)/V\}$ (in fact, we chose γ in order for the real part to exhibit noticeable oscillations). In the next section, we explain this difference, quantitatively, by appealing to the infinite antenna.

III. EXPLANATIONS VIA INFINITE ANTENNA

The infinite-antenna current $I^{(\infty)}(z)$ satisfies the well-known, analogous to (1) integral equation

$$\int_{-\infty}^{\infty} K(z - z') I^{(\infty)}(z') dz' = \frac{V}{2\zeta_c} e^{ik_c |z|}, \quad -\infty < z < \infty \quad (4)$$

(cf. [1], [2]), whose nonsolvability is due to the exponential smallness of the Fourier transform $\bar{K}(\zeta)$ of the approximate kernel $K(z)$, see eqn. (17) of the Appendix.¹ To apply Galerkin's method with pulse functions to (4), we set

$$I^{(\infty)}(z) \cong \sum_{n=-\infty}^{\infty} I_n^{(\infty)} u_n(z), \quad -\infty < z < \infty \quad (5)$$

where $u_n(z)$ ($n = 0, \pm 1, \dots$) are the pulse basis functions of finite width z_0 , with $u_0(z)$ centered at $z = 0$. Substitute (5) into (4), multiply by $u_l(z)$, and integrate with respect to z to obtain the system of equations

$$\sum_{n=-\infty}^{\infty} A_{l-n} I_n^{(\infty)} = B_l, \quad l = 0, \pm 1, \pm 2, \dots \quad (6)$$

¹When the exact kernel is used, the corresponding integral equation is solvable and, in fact, one can explicitly calculate the associated fields inside and outside the tube [2].

for the unknown basis-function coefficients $I_n^{(\infty)}$, where A_l and B_l are determined in the Appendix.

The key idea is that the system (6) is doubly infinite and Toeplitz and can therefore be solved exactly for nonzero z_0 using Fourier series, i.e., by application of the usual process of discrete deconvolution. This is done in the Appendix. Then, the Appendix determines the asymptotic behavior of $I_n^{(\infty)}$ subject to the conditions

$$\frac{z_0}{a} \ll 1, \quad \frac{n z_0}{a} = O(1), \quad |k_c| z_0 \ll 1 \quad (7)$$

The first two conditions are the same as in [1], while the third one is new. The final asymptotic result is

$$\begin{aligned} I_n^{(\infty)} \sim & -i \frac{V}{\zeta_c} \frac{\pi^3}{32\sqrt{2}} k_c z_0 \sqrt{\frac{z_0}{a}} (-1)^n \\ & \times \exp\left(\frac{a\pi}{z_0}\right) \frac{1}{\cosh\left(\frac{\pi}{2} \frac{z_0}{a} n\right)} \\ & \times \left[1 - \frac{5}{2\pi} \frac{z_0}{a} + \frac{5}{4} n \left(\frac{z_0}{a}\right)^2 \tanh\left(\frac{\pi}{2} \frac{z_0}{a} n\right) \right] \end{aligned} \quad (8)$$

As already mentioned in our Introduction, (8) is very similar to the corresponding equation in [1], namely eqn. (38) of [1]. In fact, the only difference is that the real parameters k and ζ_0 of [1] are replaced by the complex parameters k_c and ζ_c . Since (3) gives

$$\frac{k_c/\zeta_c}{k/\zeta_0} = \frac{\omega\epsilon_c}{\omega\epsilon} = 1 + i \frac{\gamma}{\omega\epsilon} \quad (9)$$

we can divide (8) by eqn. (38) of [1] to obtain

$$\frac{I_n^{(\infty)}}{V} \sim (1 + i \tan \delta) \frac{I_{n,\text{lossless}}^{(\infty)}}{V} \quad (10)$$

where $\tan \delta = \gamma/(\omega\epsilon)$ is the usual loss tangent of the surrounding medium and $I_{n,\text{lossless}}^{(\infty)}$ is the corresponding quantity for the lossless case (i.e., the basis-function coefficient determined asymptotically in [1]). While simple, we stress that (10)—which is asymptotic—was not expected beforehand. No relation similar to (10) holds far from the driving point, or when the pulse width z_0 is large. In other words, (10) is valid only subject to (7), only describes behavior near $z = 0$, and is not valid far from $z = 0$.

As $I_{n,\text{lossless}}^{(\infty)}/V$ is purely imaginary, (8) and (10) predict oscillations in both the real and the imaginary parts, with a ratio asymptotically equal to $-\tan \delta$, and with oscillations in the imaginary part asymptotically the same as in the lossless case. For parameters as in Figs. 1 and 2, Table I shows that the first few values of I_n/V are close to the values of $I_n^{(\infty)}/V$ obtained from (8). Table I also verifies (compare to Table II of [1]) that γ has negligible influence on the oscillations in the imaginary part. Our Table I (as well as many other similar results we have obtained) indicates that the oscillating values obtained via Galerkin's method for the finite antenna can be *quantitatively* estimated from our analytical/asymptotic results for the infinite antenna. We stress that our Table I is representative of what occurs within a wide range of parameter values, as long as the parameters satisfy (7).

IV. CONCLUSIONS, EXTENSIONS, FUTURE WORK

The main difficulty associated with the moment-method solutions of the usual thin-wire integral equations with the approximate kernel is known from [1]: For a sufficiently large number of basis functions, the imaginary part $\text{Im}\{I(z)/V\}$ is very large and oscillates rapidly. In the present paper, we extended this result to the case where the surrounding medium is imperfectly conducting. It was found that oscillations occur in both the real and the imaginary parts. As in the lossless case, the oscillations are not due to roundoff errors or to matrix-ill-conditioning effects: while important (e.g. the admittance matrix pertaining to Figs. 1 and 2 and Table I has a condition number equal to 5×10^8), such issues are completely separate.

As in [1], our analytical/asymptotic results for the infinite antenna help us understand the behavior of the numerical solutions for the finite one. Furthermore, many of the extensions and remarks of [1] continue to hold in the present case. For example, since $(2N+1)z_0 = 2h$ in the finite antenna, the condition $z_0 \gg a$ for oscillations near the driving point [see (7)] translates to $N \gg h/a$ for the finite antenna. Also, oscillations occur with different basis and testing functions; these, however, can give rise to different asymptotic formulas. Many of our results carry over, without modification, to Pocklington's equation. Finally, our analytical/asymptotic study is only relevant to oscillations near the driving point; for a study of oscillations near the endpoints (see our two figures), one must solve a Wiener-Hopf sum equation and (as in the lossless case [1]) this seems difficult to carry out.

We have additionally applied our methods to the so-called “extended thin-wire kernel” (see [4] for the lossless case). Our main conclusions continue to hold, while the essential benefits of the extended kernel (milder and slower oscillations) were verified via extensive numerical experiments.

Future work will focus on the *a posteriori* remedy mentioned in our Introduction. The detailed understanding obtained via (10) is expected (as in the lossless case [14], [15]) to greatly facilitate this study.

ACKNOWLEDGMENT

We thank C. Arvanitis and M. Bagakis for helping with typesetting.

V. APPENDIX

As long as k and ζ are replaced by k_c and ζ_c , eqns. (20) and (8) of [1] continue to hold, giving a closed-form expression for B_l and a single-integral expression for A_l . To solve the infinite system (6), introduce the Fourier series

$$\begin{aligned} \bar{A}(\theta) &= \sum_{l=-\infty}^{\infty} A_l e^{il\theta}, & \bar{B}(\theta) &= \sum_{l=-\infty}^{\infty} B_l e^{il\theta} \\ \bar{I}(\theta) &= \sum_{l=-\infty}^{\infty} I_l^{(\infty)} e^{il\theta} \end{aligned} \quad (11)$$

and the use the convolution theorem to obtain

$$I_n^{(\infty)} = \frac{1}{2\pi} \int_{-\pi}^{\pi} \frac{\bar{B}(\theta)}{\bar{A}(\theta)} e^{-in\theta} d\theta = \frac{1}{\pi} \int_0^{\pi} \frac{\bar{B}(\theta)}{\bar{A}(\theta)} \cos(n\theta) d\theta \quad (12)$$

TABLE I
COMPARISON OF THE FIRST 32 VALUES OF THE COMPLEX I_n/V DERIVED VIA GALERKIN'S METHOD (FOR THE FINITE ANTENNA) TO CORRESPONDING RESULTS OBTAINED VIA (8) (FOR THE INFINITE ANTENNA). THE PARAMETERS (h/λ , a/λ , ETC.) ARE THOSE OF FIGS. 1 AND 2.

n	$\text{Re}\{I_n/V\}$	$\text{Re}\{I_n^{(\infty)}/V\}$	$\text{Im}\{I_n/V\}$	$\text{Im}\{I_n^{(\infty)}/V\}$	n	$\text{Re}\{I_n/V\}$	$\text{Re}\{I_n^{(\infty)}/V\}$	$\text{Im}\{I_n/V\}$	$\text{Im}\{I_n^{(\infty)}/V\}$
0	9.56×10^2	8.95×10^2	-2.66×10^2	-2.49×10^2	16	3.54×10^1	3.58×10^1	-9.86×10^0	-9.95×10^0
1	-9.23×10^2	-8.72×10^2	2.57×10^2	2.42×10^2	17	-2.77×10^1	-2.77×10^1	7.72×10^0	7.73×10^0
2	8.37×10^2	8.07×10^2	-2.33×10^2	-2.25×10^2	18	2.17×10^1	2.16×10^1	-6.04×10^0	-6.00×10^0
3	-7.23×10^2	-7.14×10^2	2.01×10^2	1.99×10^2	19	-1.70×10^1	-1.67×10^1	4.73×10^0	4.65×10^0
4	6.02×10^2	6.08×10^2	-1.68×10^2	-1.69×10^2	20	1.33×10^1	1.30×10^1	-3.70×10^0	-3.61×10^0
5	-4.90×10^2	-5.03×10^2	1.36×10^2	1.40×10^2	21	-1.04×10^1	-1.00×10^1	2.91×10^0	2.79×10^0
6	3.93×10^2	4.07×10^2	-1.09×10^2	-1.13×10^2	22	8.17×10^0	7.78×10^0	-2.27×10^0	-2.16×10^0
7	-3.13×10^2	-3.26×10^2	8.70×10^1	9.06×10^1	23	-6.39×10^0	-6.02×10^0	1.78×10^0	1.67×10^0
8	2.47×10^2	2.58×10^2	-6.88×10^1	-7.12×10^1	24	5.01×10^0	4.66×10^0	-1.39×10^0	-1.30×10^0
9	-1.95×10^2	-2.03×10^2	5.41×10^1	5.65×10^1	25	-3.92×10^0	-3.60×10^0	1.10×10^0	1.00×10^0
10	1.53×10^2	1.59×10^2	-4.25×10^1	-4.44×10^1	26	3.08×10^0	2.78×10^0	-8.52×10^{-1}	-7.74×10^{-1}
11	-1.20×10^2	-1.25×10^2	3.34×10^1	3.47×10^1	27	-2.40×10^0	-2.15×10^0	6.73×10^{-1}	5.98×10^{-1}
12	9.40×10^1	9.74×10^1	-2.62×10^1	-2.71×10^1	28	1.89×10^0	1.66×10^0	-5.21×10^{-1}	-4.61×10^{-1}
13	-7.37×10^1	-7.60×10^1	2.05×10^1	2.11×10^1	29	-1.47×10^0	-1.28×10^0	4.14×10^{-1}	3.56×10^{-1}
14	5.77×10^1	5.92×10^1	-1.61×10^1	-1.65×10^1	30	1.16×10^0	9.88×10^{-1}	-3.18×10^{-1}	-2.75×10^{-1}
15	-4.52×10^1	-4.60×10^1	1.26×10^1	1.28×10^1	31	-9.01×10^{-1}	-7.62×10^{-1}	2.55×10^{-1}	2.12×10^{-1}

The Fourier series for $\bar{B}(\theta)$ converges by the aforementioned closed-form expression for B_l and the condition $\text{Im}\{k_c\} > 0$ of Section II. Direct summation² then gives

$$\bar{B}(\theta) = -\frac{iV}{\zeta_c} \frac{2}{k_c} \sin^2 \frac{k_c z_0}{4} \frac{\cos \frac{k_c z_0}{2} + \cos^2 \frac{\theta}{2}}{\sin \frac{\theta + k_c z_0}{2} \sin \frac{\theta - k_c z_0}{2}} \quad (13)$$

Substituting the aforementioned expression for A_l into (11) and applying the usual Poisson summation formula yields

$$\bar{A}(\theta) = \sum_{m=-\infty}^{\infty} \int_{-\infty}^{\infty} \int_0^{z_0} (z_0 - z) [K(z - xz_0) + K(z + xz_0)] dz e^{ix(\theta - 2m\pi)} dx \quad (14)$$

Let $\bar{K}(\zeta)$ denote the Fourier transform (not to be confused with our similar notation for Fourier series) of $K(z)$. Eqn. (14) can be rewritten as

$$\bar{A}(\theta) = z_0 \sum_{m=-\infty}^{\infty} \bar{K}\left(\frac{2m\pi - \theta}{z_0}\right) \frac{\sin^2 \frac{\theta}{2}}{(m\pi - \frac{\theta}{2})^2} \quad (15)$$

Integrals 2.5.25.9 and 2.5.25.15 of [35] and the detailed analytic-continuation arguments of [2] give $\bar{K}(\zeta)$ as

$$\bar{K}(\zeta) = \frac{1}{2\pi} K_0\left(a\sqrt{\zeta^2 - k_c^2}\right) \quad (16)$$

where K_0 is the modified Bessel function. Eqns. (12), (13), (15), and (16) provide the *exact* solution of the Toeplitz system (6) for *nonzero* discretization length z_0 .

²This is somewhat simpler than the corresponding step in [1], where one must additionally assume that $\text{Im}\{k\} > 0$. As a result, the integrals corresponding to those in (12) have indented integration contours.

As $z_0 \rightarrow 0$, (16) shows that $\bar{K}(\zeta)$ is exponentially small:

$$\bar{K}(\zeta) \sim \frac{1}{2} \sqrt{\frac{1}{2\pi a |\zeta|}} e^{-a|\zeta|} \quad (17)$$

We can thus approximate the denominator in the integrand of (12) by the first two terms ($m = 0$ and $m = 1$) in the sum (15) and then set $\phi = \pi - \theta$ to obtain (18), shown at the bottom of this page. As $z_0 \rightarrow 0$, the dominant contribution to the integral in (18) comes from a small interval near $\phi = 0$. Thus the contribution \int_1^π is negligible and we can change the upper integration limit in (18) from π to 1. We then replace the two instances of \bar{K} using (17) and set $x = \phi a/z_0$ to get

$$I_n^{(\infty)} \sim \frac{1}{\sqrt{2\pi}} k_c z_0 \sqrt{\frac{z_0}{a}} (-1)^n e^{\pi \frac{a}{z_0}} f\left(\frac{z_0}{a}, k_c a, n \frac{z_0}{a}\right) \quad (19)$$

where f is given by eqns. (35) and (36) of [1] with k and ζ replaced by k_c and ζ_c . Those two equations and steps identical to steps in [1] allow us to obtain the first two terms in the Taylor-series expansion of f in powers of z_0/a . Upon substituting the expression for f thus obtained into (19), we arrive at the desired asymptotic result (8).

REFERENCES

- [1] G. Fikioris and T. T. Wu, "On the application of numerical methods to Hallen's equation," *IEEE Trans. Antennas Propagat.*, vol. 49, no. 3, pp. 383-392, March 2001.
- [2] T. T. Wu, "Introduction to linear antennas," in *Antenna Theory*, R. E. Collin and F. J. Zucker, Eds. New York: McGraw-Hill, 1969, pt. I, ch.8.
- [3] P. J. Papakanellos, G. Fikioris, and A. Michalopoulos, "On the oscillations appearing in numerical solutions of solvable and nonsolvable integral equations for thin-wire antennas," *IEEE Trans. Antennas Propagat.*, vol. 58, no. 5, pp. 765-772, March 2010.

$$I_n^{(\infty)} \sim \frac{(-1)^n}{4\pi z_0} \int_0^\pi \frac{\bar{B}(\pi - \phi)/\cos^2 \frac{\phi}{2}}{\bar{K}\left(\frac{\pi - \phi}{z_0}\right)/(\pi - \phi)^2 + \bar{K}\left(\frac{\pi + \phi}{z_0}\right)/(\pi + \phi)^2} \cos n\phi d\phi \quad (18)$$

- [4] P. J. Papakanellos, P. Paschalidis, and G. Fikioris, "On the extended thin-wire kernel," *IEEE Trans. Antennas Propagat.*, vol. 64, no. 7, pp. 3180-3184, July 2016.
- [5] G. Fikioris, J. Lionas, and C. G. Lioutas, "The use of the frill generator in thin-wire integral equations," *IEEE Trans. Antennas Propagat.*, vol. 51, no. 8, pp. 1847-1854, August 2003.
- [6] G. Fikioris and C. A. Valagianopoulos, "Input admittances arising from explicit solutions to integral equations for infinite-length dipole antennas," *Progress in Electromagnetics Research*, vol. 55 (PIER 55), pp. 285-306, 2005.
- [7] I. Tachtsoglou and G. Fikioris, "Fundamentals of thin-wire integral equations with the finite-gap generator-Part I," *IEEE Trans. Antennas Propagat.*, vol. 61, no. 11, pp. 5517-5526, Nov. 2013.
- [8] I. Tachtsoglou and G. Fikioris, "Fundamentals of thin-wire integral equations with the finite-gap generator-Part II," *IEEE Trans. Antennas Propagat.*, vol. 61, no. 11, pp. 5527-5532, Nov. 2013.
- [9] G. Fikioris, P. J. Papakanellos, and H. T. Anastassiou, "On the use of nonsingular kernels in certain integral equations for thin-wire circular-loop antennas," *IEEE Trans. Antennas Propagat.*, vol. 56, no. 1, pp. 151-157, Jan. 2008.
- [10] A. McKinley, *The Analytical Foundations of Loop Antennas and Nano-Scaled Rings*. Singapore: Springer Nature Singapore, 2019.
- [11] G. Fikioris, I. Tachtsoglou, G. D. Kolezas, and T. Hatziafratis, "Unphysical moment-method solutions of an approximate integral equation of electrostatics," *IEEE Antennas and Propagation Magazine*, DOI 10.1109/MAP.2017.2686318, pp. 142-153, June 2017.
- [12] G. Fikioris and A. Papathanasopoulos, "On the thin-wire integral equations for carbon nanotube antennas," *IEEE Trans. Antennas Propagat.*, vol. 66, no. 7, pp. 3567-3576, July 2018.
- [13] P. J. Papakanellos and G. Fikioris, "A possible remedy for the oscillations occurring in thin-wire MoM analysis of cylindrical antennas," *Progress in Electromagnetics Research*, vol. 69 (PIER 69), pp. 77-92, 2007.
- [14] G. Fikioris, P. J. Papakanellos, Th. K. Mavrogordatos, N. Lafka, and D. Koulikas, "Eliminating unphysical oscillations arising in Galerkin solutions to classical integral equations of antenna theory," *SIAM J. Appl. Math.*, vol. 71, no. 2, pp. 559-585, 2011.
- [15] G. Fikioris, P. J. Papakanellos and Th. K. Mavrogordatos, "Surface-wave and superdirective aspects of effective current for linear antennas," *SIAM J. Appl. Math.*, vol. 73, no. 5, pp. 1926-1940, 2013.
- [16] Th. K. Mavrogordatos, A. Papathanasopoulos, and G. Fikioris, "An effective-current approach for Halléns equation in center-fed dipole antennas with finite conductivity," *IEEE Transactions Antennas Propagat.*, vol. 67, no. 6, pp. 3680-3687, June 2019.
- [17] R. W. P. King and G. S. Smith, *Antennas in Matter*. Cambridge, MA, USA: MIT Press, 1981.
- [18] J. H. Richmond, "Radiation and scattering by thin-wire structures in a homogeneous surrounding medium," *IEEE Trans. Antennas Propagat.*, vol. 22, no. 2, p. 365, 1974.
- [19] M. V. Shuba, G. Ya. Slepyan, S. A. Maksimenko, and G. W. Hanson, "Radiofrequency field absorption by carbon nanotubes embedded in a conductive host," *J. Appl. Phys.*, vol. 108, 114302, Dec. 2010.
- [20] J. D. Kraus and R. J. Marhefka, *Antennas for All Applications*, 3rd ed., McGraw-Hill, New York, 2002.
- [21] C. A. Balanis, *Advanced Engineering Electromagnetics*, 2nd Ed. New York, Wiley, 2012.
- [22] W. L. Stutzman and G. A. Thiele, *Antenna Theory and Design*, 3rd Ed., Wiley, New York, 2013.
- [23] C. A. Balanis, *Antenna Theory: Analysis and Design*, 4th ed., Wiley, New York, 2016.
- [24] A. R. Clark, A. P. C. Fourie, and D. C. Nitch, "Stationary, nonstationary, iterative method of moments solution schemes," *IEEE Trans. Antennas Propagat.*, 49 (2001).
- [25] G. W. Hanson, "Fundamental transmitting properties of carbon nanotube antennas," *IEEE Trans. Antennas Propagat.*, vol. 53, no. 11, pp. 34263435, 2005.
- [26] Y. Huang, W.-Y. Yin, and Q. H. Liu, "Performance prediction of carbon nanotube bundle dipole antennas," *IEEE Trans. Nanotechnology*, vol. 7, no. 3, pp. 331337, 2008.
- [27] S. D. Keller, A. I. Zaghoul, V. Shanov, M. J. Schulz, D. B. Mast, and N. T. Alvarez, "Electromagnetic simulation and measurement of carbon nanotube thread dipole antennas," *IEEE Trans. Nanotechnology*, vol. 13, no. 2, pp. 394403, 2014.
- [28] N. Fichtner, X. Zhou, and P. Russer, "Investigation of carbon nanotube antennas using thin wire integral equations," *Advances in Radio Science: ARS*, vol. 6, p. 209, 2008.
- [29] E. Forati, A. D. Mueller, P. G. Yarandi, and G. W. Hanson, "A new formulation of Pocklington's equation for thin wires using the exact kernel," *IEEE Trans. Antennas Propagat.*, vol. 59, no. 11, pp. 43554360, 2011.
- [30] G. W. Hanson, "Current on an infinitely-long carbon nanotube antenna excited by a gap generator," *IEEE Trans. Antennas Propagat.*, vol. AP-54, no. 1, pp. 76-81, Jan. 2006.
- [31] J. Hao and G. W. Hanson, "Infrared and optical properties of carbon nanotube dipole antennas," *IEEE Trans. Nanotechnol.*, vol. 5, no. 6, pp. 766-775, Nov. 2006.
- [32] R. W. P. King and C. W. Harrison, *Antennas and waves: A modern approach*, Cambridge, MA, The MIT Press, 1969, p. 167.
- [33] B. D. Popović, M. B. Dragović, and A. R. Djordjević, *Analysis and synthesis of wire antennas*, London, Research Studies Press, 1982, p. 146.
- [34] W. E. Patitz, B. C. Brock and E. G. Powell, "Measurement of dielectric and magnetic properties of soil," *Sandia National Laboratories Report SAND95-2419*, 1995, available: www.inis.iaea.org
- [35] A. P. Prudnikov, Yu. A. Brychkov, and O. I. Marichev, *Integrals and Series: Elementary Functions*, vol. 1. Amsterdam, Gordon & Breach, 1986.